Document downloaded from:

http://hdl.handle.net/10251/194986

This paper must be cited as:

Gil-Romero, J.; Tur Valiente, M.; Correcher Salvador, A.; Gregori Verdú, S.; Pedrosa, AM.; Fuenmayor Fernández, F. (2022). Hardware-in-the-loop pantograph tests using analytical catenary models. Vehicle System Dynamics. 60(10):3504-3518. https://doi.org/10.1080/00423114.2021.1962538

The final publication is available at

https://doi.org/10.1080/00423114.2021.1962538

Copyright Taylor & Francis

Additional Information

This is an Accepted Manuscript of an article published by Taylor & Francis in Vehicle System Dynamics on 3 Oct 2022, available online: https://doi.org/10.1080/00423114.2021.1962538

Hardware-in-the-loop pantograph tests using analytical catenary models

J. Gil[a], M. Tur[a], A. Correcher[b], S. Gregori[a,*], A. Pedrosa[a], F.J. Fuenmayor[a]

[a] *Instituto de Ingeniería Mecánica y Biomecánica, Universitat Politècnica de València, Camino de Vera s/n, 46022, Valencia (Spain)*
[b] *Instituto de Automática e Informática Industrial, Universitat Politècnica de València, Camino de Vera s/n, 46022, Valencia (Spain)*

Abstract

Pantograph hardware-in-the-loop (HIL) testing is an experimental method in which a physical pantograph is excited by an actuator which reproduces the movement of a virtual catenary. This paper proposes a new method that uses analytical catenary models for HIL tests. The approach is based on an iterative scheme until achieving a steady-state regime. Some of the method's advantages include its ability to consider the delay in the control and communication system and its applicability to a wide range of analytical catenary models. The proposed algorithm was validated both numerically and experimentally. The experimental results obtained in the HIL pantograph tests were compared with those obtained from pure numerical simulations using a linear pantograph model and showed good accuracy with pantograph running at different speeds.

Keywords: Hardware-In-the-Loop, Analytical catenary model, Steady-state response, Pantograph

*Corresponding author.

1. Introduction

High-speed locomotives collect current through the sliding contact between the pantograph and the railway catenary, which is composed of overlapping independent sections of about 1 km in length (see Fig. 1). Each section contains a messenger wire and droppers that hold the contact wire, which interacts with the collector strips on the pantograph, at the appropriate height. Messenger and contact wires are supported by brackets and posts at regular intervals, called spans.

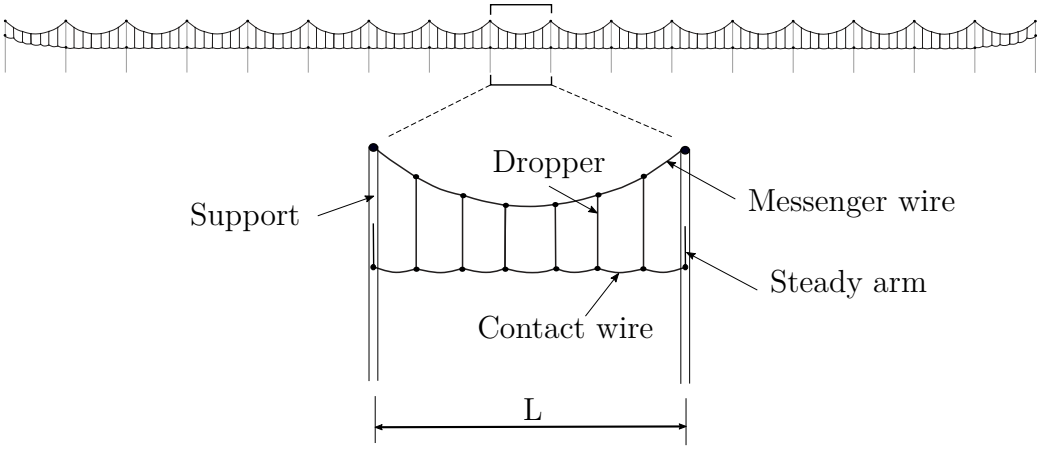

Figure 1: *Scheme of a catenary section and detail of a single span.*

The contact force produced in the pantograph-catenary dynamic interaction plays an important role in assessing the quality of the power supply. This contact force reaches a steady-state regime in the central spans of each catenary section, where the catenary can be assumed a periodic structure with repetitive spans. Both numerical and experimental methods are now widely used to assess the contact force. Several computer programs are able to simulate the pantograph-catenary dynamic interaction [1], which is espe-

cially useful in the early stages of the design process. In-line tests are also made with instrumented pantographs to measure experimentally the pantograph interaction force. These tests are required for the validation of a given pantograph-catenary couple; in Europe for example the requirements are provided by the EN 50317 standard [2].

To reduce the number of costly in-line tests, pantograph Hardware-In-the-Loop (HIL) lab tests have arisen as an appealing cheaper alternative, in which the catenary is replaced by an actuator that interacts with a real pantograph. The actuator movements simulate the position of the catenary contact point, which depends on the catenary's dynamic behaviour and the measured interaction force. The catenary model should be as realistic as possible but at the same time must be solved in real-time, which is usually managed by the use of simplified catenary models instead of more complex finite element models with direct time integration.

The first works that proposed a pantograph HIL test rig were [3, 4] using a finite length catenary model based on a truncated modal approach to study the influence of different parameters on the pantograph-catenary dynamic interaction. Another HIL set-up for pantograph dynamics evaluation was proposed in [5], in which a hydraulic actuator reproduces the vertical movement of a very simple catenary model composed of three spans. This model was upgraded in [6] with the consideration of the non-linear dropper behaviour and in [7] by incorporating lateral movement in the test rig to simulate the catenary stagger. In [8], a linear model of the catenary with 3D Euler-Bernoulli beams is used in combination with a moving coordinates formulation and absorbing boundary layers at both ends of the catenary model.

All the catenary models used in the above mentioned references are finite length models which need the use of specific boundary conditions to perform HIL tests.

In this work we propose a new method of performing pantograph HIL tests using analytical catenary models. In general terms, these analytical models provide the steady-state solution at the central spans of a catenary section with different degrees of approximation. One of the simplest models is found in [9], in which the catenary is modelled as a single and two-degrees-of-freedom system with periodically time-varying mass and stiffness. A more complex model was presented in [10], in which an infinite string with visco-elastic support is used to obtain the stationary response of lumped-parameter moving models coupled to the string. The even more complex infinite string models include periodic discrete elements, such as in [11] or [12], in which a two-level infinite catenary model, composed of an upper and lower string joined by periodic supports and dampers, is simulated along with a pantograph modelled by a harmonic point-load. Similar models can also be found in the literature, such as that proposed in [13], which is composed of several finite strings and is used to study the catenary wave propagation and reflection phenomena. Of the wide variety of analytical catenary models, we here use that proposed in [14], which considers the main catenary dynamic features and the initial contact wire height profile.

The paper is organised as follows. After this introduction, the analytical catenary model chosen for this work is briefly described in Section 2. The algorithm proposed to perform steady-state HIL tests is presented and validated in Section 3. Section 4 describes the test rig components and the

control system. An experimental validation of the setup and some HIL tests results are provided in Section 5, while the concluding remarks are given in Section 6.

2. Analytical catenary model

In this paper we present the results obtained with a particular analytical catenary model, but it should be noted that the proposed method can also be applied to other analytical models, as long as they provide the response of the catenary contact point under a harmonic load moving at a constant velocity.

2.1. Dynamic behaviour

The model chosen for this work is an improved version of the one proposed by Roy et al. [10], which is based on the response of a viscoelastically supported infinite string excited by a moving load with uniform speed. This model is schematically depicted in Fig. 2 and was analysed in [14], in which a good agreement was obtained with the steady-state results of Finite Element simulations. For the sake of completeness, here we summarise the main features of the model. It is composed of an axially loaded infinite string, with linear density μ and initial traction T, supported by a continuous visco-elastic layer of stiffness $\bar{k}$ per unit of length. A Kelvin-Voigt damping model of coefficients α and β considers the energy dissipation similarly to Finite Element models.

The string model subjected to a general load $p(x,t)$ is governed by the

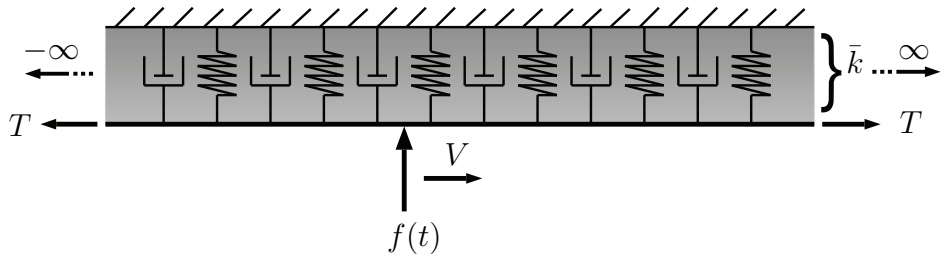

Figure 2: *Analytical string model with visco-elastic support under a moving load.*

following equation:

$$\mu\frac{\partial^2 u}{\partial t^2} - T\frac{\partial^2 u}{\partial x^2} + \left(\alpha\mu + \beta\bar{k}\right)\frac{\partial u}{\partial t} - \beta T\frac{\partial}{\partial t}\left(\frac{\partial^2 u}{\partial x^2}\right) + \bar{k}u = p(x,t) \qquad (1)$$

where $u = u(x,t)$ is the vertical displacement of the string.

As depicted in Fig. 2, for a concentrated load moving at constant speed V, the right-hand side term of Eq. (1) can be expressed as:

$$p(x,t) = f(t)\ \delta(x - Vt) \qquad (2)$$

where δ denotes the *Dirac* function.

If the load is a harmonic function of frequency ω, $f(t) = F_0 e^{i\omega t}$, the closed solution of Eq. (1) for any point x and time t, $u(x,t)$, is obtained using the method proposed in [10, 14]. The steady-state response of the contact point of an ideally infinite catenary under harmonic excitation can thus be written as:

$$u_c(t) = u(Vt,t) = \frac{-iF_0 e^{i\omega t}}{\lambda\left(k_1(\omega) - k_2(\omega)\right)\left(k_1(\omega) - k_3(\omega)\right)} \qquad (3)$$

in which k_1, k_2, k_3 and λ depend on the excitation frequency (ω) and other model parameters (T, V, μ, $\bar{k}$, α, β) as defined in Appendix A.

This response can be characterised by the Frequency Response Function (FRF) H_s, which is defined as the ratio between the vertical displacement

and the harmonic force applied at the contact point:

$$H_s(\omega) = \frac{u_c(t)}{F_0 e^{i\omega t}} = \frac{-i}{\lambda \left(k_1(\omega) - k_2(\omega)\right)\left(k_1(\omega) - k_3(\omega)\right)} \tag{4}$$

2.2. Contact wire geometry

The contact wire height profile plays an important role in the dynamic behaviour of the pantograph-catenary system [15, 16, 17, 18]. The static configuration of the catenary that results from the stringing process can be obtained by different methods. For example, semi-analytical methods are used in [19] or a method based on a Finite Element (FE) model was proposed in [20]. Here we use a non-linear FE model [21] to obtain the height of the contact wire $z_0(x)$ in a reference catenary span of length L (see Fig. 3 and Fig. 1).

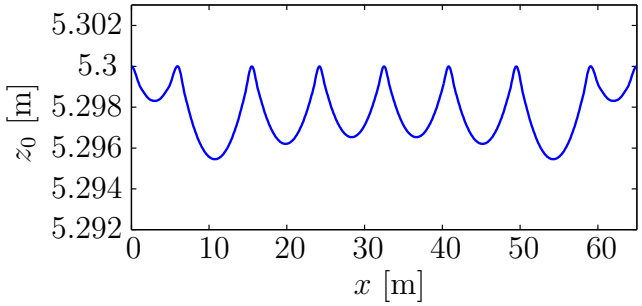

Figure 3: *Catenary contact wire height profile along a span.*

2.3. Contact point height calculation

Thanks to the linearity of the analytical model (Eq. (1)), we can obtain the contact wire height $z_c(t)$ that sees the pantograph moving at speed V as the sum of the static position and the displacement due to the moving

interaction load:

$$z_c(t) = z_0(Vt) + u_c(t) \tag{5}$$

where $z_0(Vt)$ is computed in the moving contact point.

We assume that the same span is infinitely repeated, so that z_0 is considered L-periodic of period $T = L/V$. The contact force from the steady-state response of the pantograph-catenary interaction will therefore be repeated every span, i.e. $f(t)$ in Eq. (2) will be a time periodic function of period T, as will also the displacement of the contact wire $u_c(t)$. As a consequence, the steady position of the catenary $z_c(t)$ is also a periodic function.

In a HIL test the contact force is measured at a constant rate $f_s = 1/\Delta t$, Δt being the time increment. Let us assume that the stationary interaction force is known for a whole span, $f_c(t_n) = f_c(n\Delta t)$ for $n = 0, \ldots, N-1$, in which $N = L/(V\Delta t)$. This N-periodic discrete force can be shifted to the frequency domain by applying the Discrete Fourier Transform (DFT):

$$F_c(\omega_k) = \sum_{n=0}^{N-1} f_c(t_n)\, e^{-i\omega_k n\Delta t} \tag{6}$$

in which the discrete frequencies are:

$$\omega_k = k\frac{2\pi}{N\Delta t} \quad k = 0, \ldots, N-1 \tag{7}$$

The steady-state response of the catenary is directly obtained in the frequency domain with the FRF (Eq. (4)) as:

$$U_c(\omega_k) = H_s(\omega_k)F_c(\omega_k) \tag{8}$$

Applying Eq. (5) in the frequency domain, the total contact point height can be computed:

$$Z_c(\omega_k) = Z_0(\omega_k) + U_c(\omega_k) \tag{9}$$

in which

$$Z_0(\omega_k) = \sum_{n=0}^{N-1} z_0(Vn\Delta t)\, e^{-i\omega_k n\Delta t} \tag{10}$$

Finally, the Inverse Discrete Fourier Transform (IDFT) is used to return to the time domain. Given that $f_c(t_n)$ is a real sequence and $H_s(\omega)$ exhibits Hermitian symmetry, we can write:

$$z_c(t_n) = \frac{1}{N}\left(Z_c(\omega_0) + 2\sum_{k=1}^{\frac{N-1}{2}} \mathrm{Re}\left(Z_c(\omega_k)\, e^{i\omega_k n\Delta t}\right)\right) \tag{11}$$

3. Steady-state HIL test method

The previous section showed how to compute the steady-state height of the contact point in a whole span of the catenary if the stationary contact force is known in advance. Here we propose a method of achieving the steady state (force and displacement) if the virtual catenary model interacts with a physical pantograph and the contact force is measured every time step t_n.

Fig. 4 shows a scheme of the proposed HIL test strategy. The catenary contact point is replaced by a linear actuator that imposes the height of the contact wire $z_c(t_n)$ computed by the analytical catenary model in every time step (Eq. (11)). The aim of the test is to simulate the interaction of the pantograph travelling at constant velocity V with the virtual catenary model, which is composed of an infinite sequence of equal spans of length L.

The idea behind the proposed method is to obtain iteratively the response of the contact point in the current virtual span b using the force measured in the previous one $b-1$ by means of the equations given in Section 2.3, in which the external force was assumed to be known. We define here the following variables:

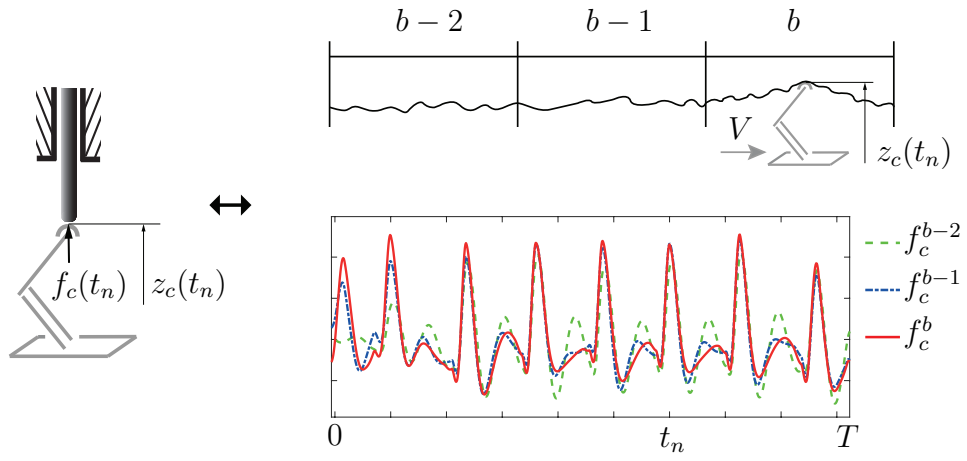

Figure 4: *Scheme of HIL test. From left to right, actuator with pantograph and the measured contact force in three successive virtual spans.*

- $f_c^b(t_n)$, $z_c^b(t_n)$: Contact force measured in the current virtual span at time $t_n = n\Delta t$, for $n = 0, \ldots, N-1$, and height of the contact point imposed.

- $f_c^{b-1}(t_n)$: Contact force measured in the previous virtual span, with t_n referring to the relative time in that span. Note that t_n is rebooted at the beginning of every virtual span.

- $F_c^{b-1}(\omega_k)$: DFT of the contact force in the previous virtual span.

3.1. Full virtual span iteration

We first define a more intuitive algorithm to better understand the final method proposed. The contact wire height of the current virtual span $z_c^b(t_n)$ is predicted by the measurements of the contact force in the previous one $f_c^{b-1}(t_n)$, following the method described in Section 2.3. The algorithm is initialised assuming null force $f_c^0(t_n)$ on the initial virtual span, so that

the predicted height of the contact point $z_c^1(t_n)$ matches the static height of the contact wire $z_0(t_n)$ (Fig. 3). The linear actuator will prescribe this contact point height in the next virtual span and a new contact force will be measured. The test runs until the contact force measured is equal (with an admissible error) in two consecutive spans.

3.2. Single step iteration

The previous strategy can be implemented more efficiently if the measured contact force is updated every time step in the current virtual span instead of every whole span. As shown in Section 3.3, with this strategy the convergence is achieved very quickly after the pantograph interacts with a few virtual spans.

To obtain the contact wire height in a given time step t_n of the current virtual span, we make a calculation block of N contact force values composed of the force already measured in the current virtual span $f_c^b(t_m)$ for $m = 0, \ldots, n$, and the force measured in the previous virtual span $f_c^{b-1}(t_m)$ for time steps $m = n+1, \ldots, N-1$. The missing contact force values needed to complete the current virtual span are fulfilled with those of the previous one.

The DFT of the contact force $F_c^n(\omega_k)$ of the calculation block of time step t_n can be obtained from Eq. (6) as:

$$F_c^n(\omega_k) = \sum_{m=0}^{n} f_c^b(t_m) e^{-i\omega_k m\Delta t} + \sum_{m=n+1}^{N-1} f_c^{b-1}(t_m) e^{-i\omega_k m\Delta t} \tag{12}$$

Eq. (12) can be rewritten in incremental form as:

$$F_c^n(\omega_k) = F_c^{n-1}(\omega_k) + \Delta F_c^n(\omega_k) \qquad k = 0, \ldots, N-1 \tag{13}$$

in which F_c^{n-1} contains the frequency content of the contact force computed in the previous time step t_{n-1} and the increment term $\Delta F_c^n(\omega_k)$ is computed from:

$$\Delta F_c^n(\omega_k) = \alpha \left(f_c^b(t_n) - f_c^{b-1}(t_n) \right) e^{-i\omega_k n \Delta t} \qquad k = 0, \ldots, N-1 \tag{14}$$

The stabilisation parameter $\alpha \in [0, 1]$ is introduced here to ensure convergence in exchange for increasing the time in which the steady state is reached.

The displacement of the contact point $U_c^n(\omega_k)$ caused by the force obtained from Eq. (13) is obtained by applying Eq. (8). The frequency content of the contact point height $Z_c^n(\omega_k)$ is then directly computed by Eq. (9). Finally, the contact wire height at time t_n, which will be imposed by the linear actuator, is transformed to the time domain according to Eq. (11).

Remark. *The proposed method has the advantages of low computational cost and low memory requirements, which make it suitable for HIL tests. The formulation includes the entire frequency content (harmonics $k = 0, \ldots, N-1$). Given that pantograph-catenary dynamics can be computed using frequencies from 0 to ω_{max}, the computational cost of the method can be further reduced by computing the solution for the range of frequencies $k = 0, \ldots, N_{cut} - 1$, in which $N_{cut} < N$ is the index associated with the maximum frequency:*

$$N_{cut} = \frac{N \Delta t}{2\pi} \omega_{max}$$

3.3. Numerical validation

Before moving to the real HIL tests, a computational reproduction of a HIL test was performed to demonstrate the the proposed method's theoretical validity, in which the measured force was replaced by the reaction force

obtained from the time integration of a linear lumped-parameter pantograph model with the contact point height imposed on the pantograph collector. The parameters used to define the analytic catenary model shown in Table 1 were taken from [14], in which they were appropriately tuned according to a realistic FEM catenary model.

Table 1: *Parameters of the analytical catenary model.*

L (m)	T (N)	μ (kg/m)	$\bar{k}$ (N/m^2)	α (s^{-1})	β (s)
65	31500	1.4735	51.15	0.0125	10^{-4}

This computational test was first used to show the effect of the stabilisation parameter α on the solution. Fig. 5 shows the contact force obtained for three different values of α along seven virtual spans with a pantograph travelling speed of $V = 250$ km/h. It can be seen that the higher the α the faster the convergence to the steady state. However, as an excessively high value for this parameter could produce instabilities in a real HIL test, a balance must be experimentally achieved between convergence speed and stability.

Since the method was verified as converging, it was important to check whether it converged to the correct solution, for which the result of this computational HIL test was compared to that of the direct method briefly introduced in Section 2 and fully available in [14]. Fig. 6 shows the contact force in a full span. Note that the converged solution of the proposed algorithm perfectly matches that obtained from the direct method, which corroborates the validity of the proposed algorithm.

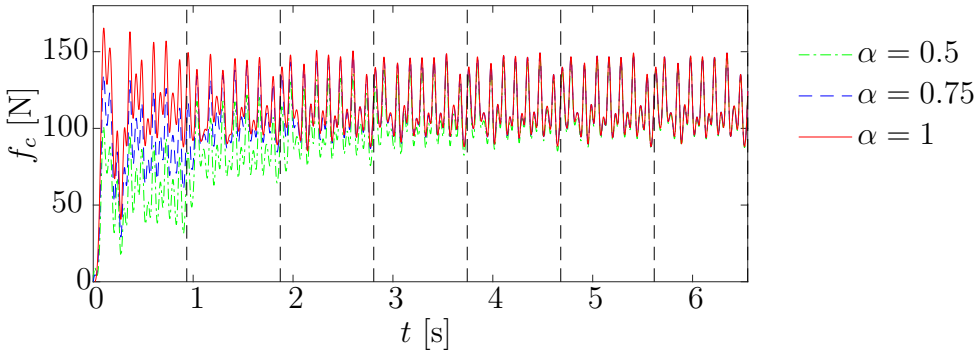

Figure 5: *Contact force in the computational HIL test with different values of the stabilisation parameter α along seven virtual spans at 250 km/h. Virtual spans are shown by vertical dashed lines.*

4. HIL test rig

The main components of the HIL test rig are depicted in Fig. 7. The contact force on each collector strip of the pantograph is measured by means of a load cell. This signal is filtered and conditioned and finally acquired by the National Instruments® cRio-9040 real-time controller in which the analytical catenary model runs to provide the contact point height that fulfils the linear actuator (LinMot® 70x400U) to simulate the catenary movement.

The contact point height is set as a reference for the servo drive LinMot® E1400, which drives the linear actuator, via Ethernet UDP communication. This servo includes a PID closed loop control of the motor position which is configured to reach the desired position using an acceleration and velocity-limited motion profile.

All these cycle tasks are shown schematically in Fig. 8. The contact force F_c between the linear actuator and the pantograph is measured, filtered

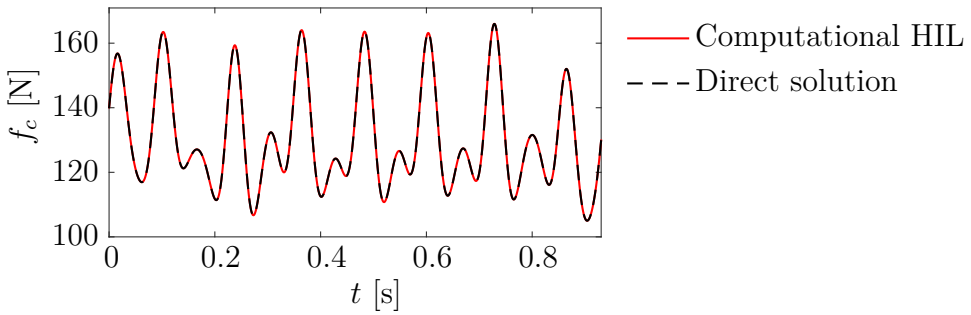

Figure 6: *Comparison of contact force obtained from the proposed algorithm and from the direct method presented in [14] for a pantograph running at 250 km/h.*

and sampled to feed the catenary model which provides the contact point height z_c every $\Delta t = 1$ ms. However, communications between the real time controller and the motor servo drive cannot take place at this rate, so that one value of every N_{com} values of z_c is sent to LinMot servo drive. For the tests described here $N_{\text{com}} = 8$ was used to ensure communications without any data loss. The value received by LinMot z_{com} is set as the new reference and the controller tries to reach this reference by generating a set of intermediate reference points, at a rate of 0.3125 ms, linearly interpolated from z_{com} and the previous reference z_{old}. The LinMot servo drive uses a PID controller, which works at a higher rate, to fulfil these intermediate references.

It is important to emphasise that the whole loop described in Fig. 8 requires a certain time to be accomplished. We can define the overall delay of the test rig, $\delta = N_\delta \Delta t$, as the time spent from when the force is measured until the computed contact point height is reached by the linear actuator. This value calculated both theoretically and experimentally gave a result of approximately 19 ms. Accounting for the test rig delay in the HIL tests is

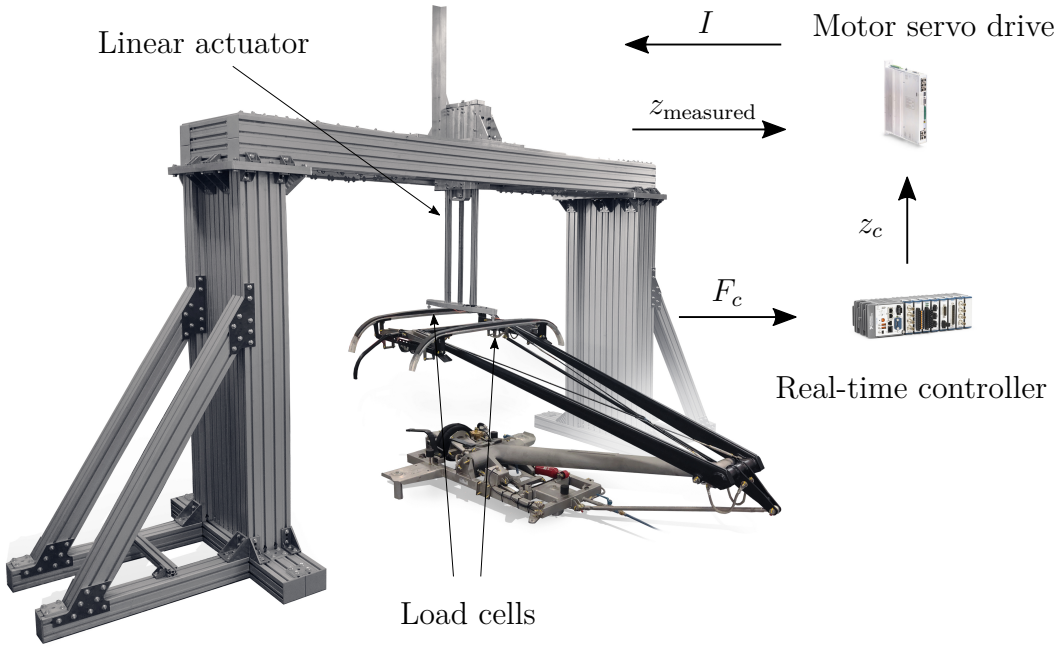

Figure 7: *HIL test rig.*

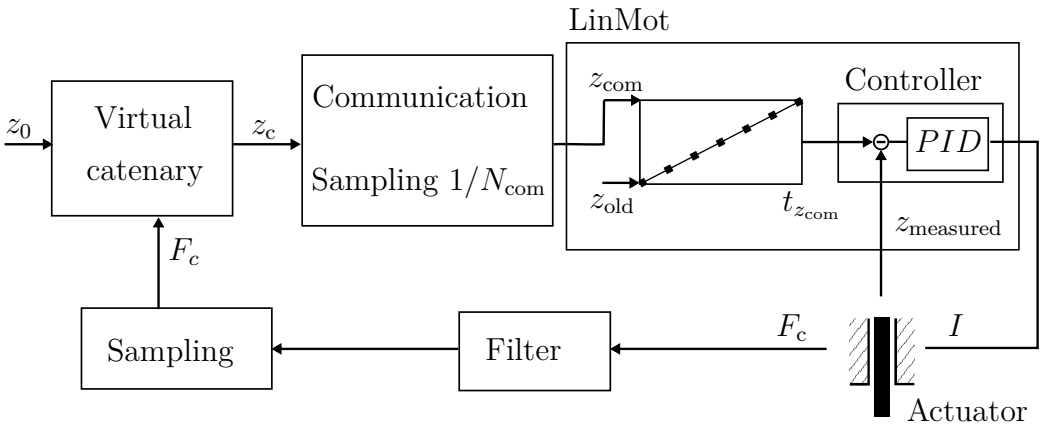

Figure 8: *Simulation cycle of tasks in HIL test.*

crucially important because omitting this step could modify the final response or even make it unstable.

One of the advantages of using analytical catenary models is the ease of dealing with the delay in the test rig. The height of the contact point can be obtained in any time step, so that if the test rig delay is known, the response of the catenary model can be obtained N_δ time steps in advance, meaning that the actuator reaches this position at the proper time.

For this end, the missing force values needed to complete the current virtual span b are assumed to be equal to the previous virtual span $b-1$. For example, if we have measured the contact force at time t_n and we want to obtain the contact point height at t_m for $m > n$, the force values between t_{n+1} and t_m, $f_c^b(t_{n+1}^m)$, are chosen as $f_c^{b-1}(t_{n+1}^m)$. As the test converges to the steady state, with this strategy the contact force will tend to be repetitive from one span to the next and the error of this assumption will thus tend to disappear.

The contact point height calculated from Eq. (11) only needs to be modified with the advanced time required:

$$\bar{z}_c(t_n) = \frac{1}{N}\left(Z_c(\omega_0) + 2\sum_{k=1}^{\frac{N-1}{2}} \mathrm{Re}\left(Z_c(\omega_k)e^{i\omega_k(n+N_\delta)\Delta t}\right)\right) \tag{15}$$

5. Experimental results

This section contains some experimental results obtained from the HIL test rig. The experimental validation of the control system and the overall performance of the test rig was first obtained by means of a benchmark test in which the pantograph was replaced by a mass. The results of the HIL tests

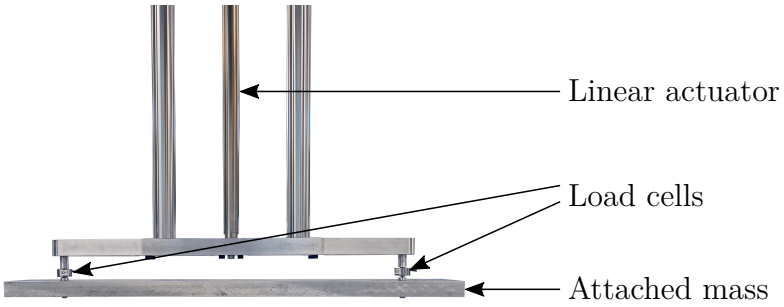

Figure 9: *Mass attached to the linear actuator for the validation test.*

with a real pantograph were then shown and compared with the analytical solution obtained from simulations with a linear pantograph model.

5.1. Experimental validation

In order to validate the control system and the proper operation of the HIL test rig, an experimental validation test was carried out in which the pantograph was replaced by a mass of 5.29 kg directly attached to the linear actuator, as shown in Fig. 9. This simple system can be modelled very accurately to obtain the analytical solution of its interaction with the catenary model.

This analytical solution is depicted in Fig. 10 when the mass is virtually moving at 300 km/h along with the contact force obtained from the HIL test rig. The experimental results include the contact force measured in the 10 last virtual spans to verify that the steady state has been achieved using the stabilisation parameter $\alpha = 0.1$. The contact force measured is filtered at 30 Hz with an analogical low-pass filter and the catenary response is computed with the first 20 harmonics ($N_{cut} = 20$) including frequencies up

to 25 Hz. Finally, the contact forces shown in Fig. 10 are low-pass filtered to 25 Hz with a digital filter.

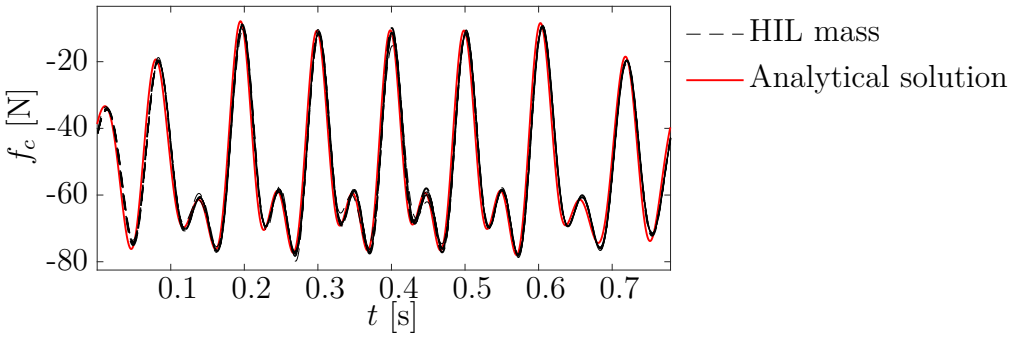

Figure 10: *Comparison of the contact force in the mass HIL test (10 spans overlapped) at 300 km/h with the analytical solution.*

As shown in Fig. 10, the experimental results are almost identical to the analytical solution, indicating a completely satisfactory experimental validation. Note that in this case the contact force has negative values because the attached mass pulls the load cells down, unlike the pantograph, which pushes them up.

5.2. Pantograph HIL tests

This section gives the results and an analysis of the pantograph HIL simulation with the same conditions to those used in the validation HIL test of Section 5.1. The contact force obtained for the last 10 virtual spans is shown in Fig. 11 with the pantograph running at 200, 225, 250, 275 and 300 km/h and with the stabilisation parameter α between 0.05 and 0.1. The number of harmonics N_{cut} included in the response varies from 30 (200 km/h)

to 20 (300 km/h) to ensure that the frequency content of the response reaches up to 25 Hz.

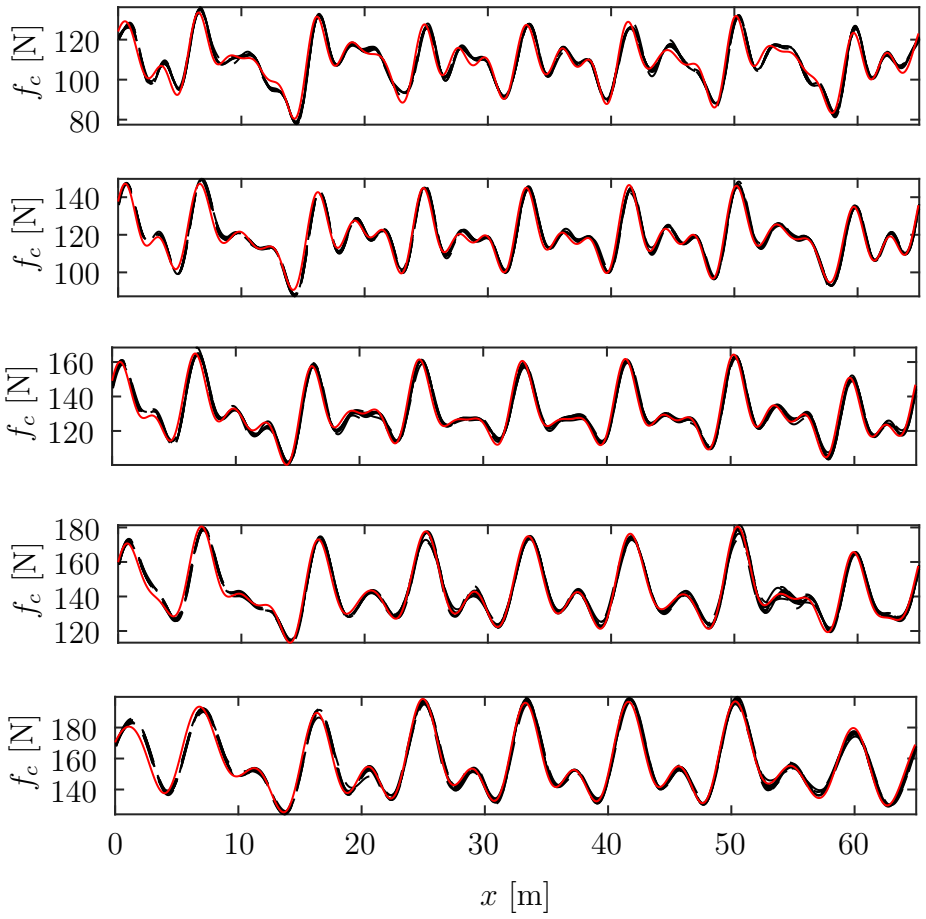

Figure 11: *Comparison of the contact force obtained from the pantograph HIL test (10 spans overlapped in black) and the analytical solution with a linear pantograph model (red curves). Tests performed at 200, 225, 250, 275 and 300 km/h from top to bottom.*

The repeatability of these 10 curves of every tests verifies that the tests

have converged to the steady-state solution. This contact force is also compared in Fig. 11 with the analytical solution obtained when using a linear lumped-parameter pantograph model showing the great similarity between them.

Some additional tests have been executed at different pantograph velocities and the standard deviation σ of the contact force is plotted in Fig. 12. Again, the experimental tests show a good agreement with the analytical solution obtained by using a linear pantograph model.

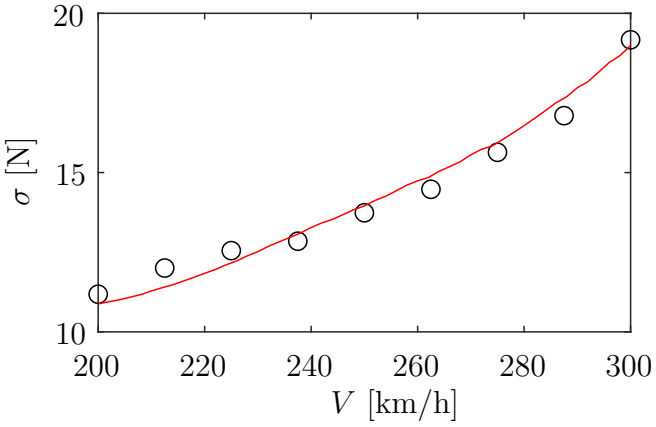

Figure 12: *Comparison of the standard deviation of the contact force obtained from pantograph HIL tests (black circles) and the analytical solution with a linear pantograph model (red curve).*

6. Conclusions

This paper defines a HIL test rig in which a physical pantograph interacts with a linear actuator that emulates the catenary dynamic behaviour,

together with an algorithm to perform HIL pantograph tests with analytic catenary models to obtain the steady-state pantograph-catenary dynamic interaction. Although a very simple string catenary model was used in this work to illustrate the proposed method, it is important to note that this strategy is applicable to a wide range of analytical catenary models provided that the Frequency Response Function can be obtained under a harmonic load travelling at constant speed. With this type of analytical catenary models there is no need to avoid boundary effects and delays in measurement and signal transmission are easily dealt with.

Furthermore, the use of a simple analytical model in HIL pantograph tests can be a useful tool to check the validity of a given pantograph model or to compare the performance of different pantographs. In this work we proved the validity of a fitted linear model of the pantograph. However, if high fidelity is required, more realistic analytical models can be used with the proposed method.

A benchmark HIL test was performed in which the pantograph was replaced by a mass directly attached to the linear actuator to validate the whole performance of the test rig and the control system. The results obtained in this reference test were then compared with the analytical response of the mass interacting with the analytical catenary model. The delay produced since the contact force is measured until the linear actuator achieves the specified height was considered in this experimental validation.

We also provide the results of the HIL tests on a physical pantograph, which show a good convergence to the steady-state solution. In general, there is good agreement between the contact force obtained from these tests and

the analytical results when using a linear pantograph model.

Acknowledgements

The authors would like to acknowledge the financial support received from the Spanish Ministry of Economy, Industry and Competitiveness [TRA2017-84736-R].

Appendix A. String catenary model solution

The string catenary model used in this work was presented in [14]. This model is governed by Eq. (1) whose solution provides the following vertical displacement of the string:

$$u(x,t) = \begin{cases} iF_0 \sum\limits_p \dfrac{e^{-i(k_p(\omega)(x-Vt)-\omega t)}}{\lambda \prod\limits_{r\neq p}(k_p(\omega)-k_r(\omega))}; & x-Vt \leq 0 \\ -iF_0 \sum\limits_q \dfrac{e^{-i(k_q(\omega)(x-Vt)-\omega t)}}{\lambda \prod\limits_{r\neq q}(k_q(\omega)-k_r(\omega))}; & x-Vt > 0 \end{cases} \tag{A.1}$$

in which $k_p(\omega)$ are the poles with a positive imaginary part and $k_q(\omega)$ are the poles with a negative imaginary part. They are:

$$\begin{aligned} k_1(\omega) &= -\frac{\eta}{3\lambda} - \frac{\sqrt[3]{2}Q}{3\lambda S} + \frac{S}{3\sqrt[3]{2}\lambda} \\ k_2(\omega) &= -\frac{\eta}{3\lambda} - \left(-\frac{1}{2} + \frac{i\sqrt{3}}{2}\right)\frac{\sqrt[3]{2}Q}{3\lambda S} + \left(-\frac{1}{2} - \frac{i\sqrt{3}}{2}\right)\frac{S}{3\sqrt[3]{2}\lambda} \\ k_3(\omega) &= -\frac{\eta}{3\lambda} - \left(-\frac{1}{2} - \frac{i\sqrt{3}}{2}\right)\frac{\sqrt[3]{2}Q}{3\lambda S} + \left(-\frac{1}{2} + \frac{i\sqrt{3}}{2}\right)\frac{S}{3\sqrt[3]{2}\lambda} \end{aligned} \tag{A.2}$$

being

$$
\begin{aligned}
S &= \sqrt[3]{R + \sqrt{4Q^3 + R^2}} \\
Q &= 3\lambda\tau - \eta^2 \\
R &= -2\eta^3 + 9\eta\lambda\tau - 27\lambda^2\sigma
\end{aligned}
\tag{A.3}
$$

and

$$
\begin{aligned}
\lambda &= i\beta TV \\
\eta &= T - \mu V^2 + i\beta T\omega \\
\tau &= i\left(\alpha\mu + \beta\bar{k}\right)V - 2\mu V\omega \\
\sigma &= \bar{k} + i\left(\alpha\mu + \beta\bar{k}\right)\omega - \mu\omega^2
\end{aligned}
\tag{A.4}
$$

References

[1] S. Bruni, J. Ambrosio, A. Carnicero, Y. H. Cho, L. Finner, M. Ikeda, S. Y. Kwon, J. P. Massat, S. Stichel, M. Tur, The results of the pantograph-catenary interaction benchmark, Vehicle System Dynamics 53 (3) (2015) 412–435.

[2] EN 50317, Railway applications. Current collection systems. Requirements for and validation of measurements of the dynamic interaction between pantograph and overhead contact line, European Committee for Electrotechnical Standardization (2012).

[3] W. Zhang, G. Mei, X. Wu, Z. Shen, Hybrid simulation of dynamics for the pantograph-catenary system, Vehicle System Dynamics 38 (6) (2002) 393–414.

[4] W. Zhang, G. Mei, X. Wu, L. Chen, A study on dynamic behaviour of pantographs by using hybrid simulation method, Proceedings of the Institution of Mechanical Engineers, Part F: Journal of Rail and Rapid Transit 219 (3) (2005) 189–199.

[5] A. Collina, A. Facchinetti, F. Fossati, F. Resta, Hardware in the loop test-rig for identification and control application on high speed pantographs, Shock and Vibration 11 (2004) 445–456.

[6] F. Resta, A. Facchinetti, A. Collina, G. Bucca, On the use of a hardware in the loop set-up for pantograph dynamics evaluation, Vehicle System Dynamics 46 (S1) (2008) 1039–1052.

[7] A. Facchinetti, M. Mauri, Hardware-in-the-loop overhead line emulator for active pantograph testing, IEEE Transactions on Industrial Electronics 56 (10) (2009) 4071–4078.

[8] A. Schirrer, G. Aschauer, E. Talic, M. Kozek, S. Jakubek, Catenary emulation for hardware-in-the-loop pantograph testing with a model predictive energy-conserving control algorithm, Mechatronics 41 (2017) 17 – 28.

[9] T. Wu, M. Brennan, Basic analytical study of pantograph-catenary system dynamics, Vehicle System Dynamics 30 (6) (1998) 443–456.

[10] A. D. S. Roy, G. Chakraborty, Coupled dynamics of a viscoelastically supported infinite string and a number of discrete mechanical systems moving with uniform speed, Journal of Sound and Vibration 415 (2018) 184–209.

[11] P. Belotserkovskiy, Forced oscillations and resonance of infinite periodic strings, Journal of Sound and Vibration 204 (1) (1997) 41 – 57.

[12] A. Metrikine, A. Bosch, Dynamic response of a two-level catenary to a moving load, Journal of Sound and Vibration 292 (3) (2006) 676 – 693.

[13] Z. Liu, F. Duan, Z. Xu, X. Lu, Wave propagation analysis in high-speed railway catenary system subjected to a moving pantograph, Applied mathematical modelling. 59 (2018) 20–38.

[14] J. Gil, S. Gregori, M. Tur, F. Fuenmayor, Analytical model of the pantograph–catenary dynamic interaction and comparison with numerical simulations, Vehicle System Dynamics (2020) 1–24.

[15] M. Aboshi, M. Tsunemoto, Installation guidelines for shinkansen high speed overhead contact lines, Quarterly Report of Railway Technical Research Institute 52 (2011) 230–236.

[16] O. V. Van, J.-P. Massat, C. Laurent, E. Balmes, Introduction of variability into pantograph–catenary dynamic simulations, Vehicle System Dynamics 52 (10) (2014) 1254–1269.

[17] S. Gregori, M. Tur, J. E. Tarancón, F. J. Fuenmayor, Stochastic monte carlo simulations of the pantograph–catenary dynamic interaction to allow for uncertainties introduced during catenary installation, Vehicle System Dynamics 57 (4) (2019) 471–492.

[18] S. Gregori, M. Tur, E. Nadal, F. J. Fuenmayor, An approach to geometric optimisation of railway catenaries, Vehicle System Dynamics 56 (8) (2018) 1162–1186.

[19] O. Lopez-Garcia, A. Carnicero, V. Torres, Computation of the initial equilibrium of railway overheads based on the catenary equation, Engineering Structures 28 (10) (2006) 1387 – 1394.

[20] M. Tur, E. García, L. Baeza, F. Fuenmayor, A 3D absolute nodal coordinate finite element model to compute the initial configuration of a railway catenary, Engineering Structures 71 (2014) 234–243.

[21] M. Tur, L. Baeza, F. Fuenmayor, E. García, Pacdin statement of methods, Vehicle System Dynamics 53 (3) (2015) 402–411.